Chemical sputtering yields of carbon based materials at high ion flux densities

H. Grote[1]*, W. Bohmeyer[1], P. Kornejew[1], H. -D. Reiner[1], G. Fussmann[1], R. Schlögl[2], G. Weinberg[2] and C. H. Wu[3]

[1] Max-Planck-Institut für Plasmaphysik, Bereich Plasmadiagnostik, EURATOM Association, Mohrenstr. 41, D-10117 Berlin, Germany

[2] Department of Inorganic Chemistry, Fritz-Haber-Institute of the MPG, Faradayweg 4-6, 14195 Berlin, Germany

[3] NET Team, Max-Planck-Institut für Plasmaphysik, EURATOM Association, Boltzmannstr. 2, D-85748 Garching, Germany

* Corresponding author: e-mail hig@ipp-garching.mpg.de, phone +49 89 3299 2128, fax +49 89 3299 12 12

Abstract

Graphite and advanced carbon fiber composites (CFC) are widely used inside the vacuum vessel of magnetic fusion devices. However, erosion by chemical sputtering via hydrocarbon formation might limit their application as target material in future machines like ITER. The first systematic study of the chemical erosion of graphite and different CFCs (including a silicon-doped one) as a function of ion flux density in the range of 1.4×10^{21}–5×10^{22} m^{-2} s^{-1} was performed in the plasma generator PSI-1. The results of three different analysis methods agree within about 40%. No differences in the chemical erosion yields between hydrogen and deuterium exposures are found for the various materials. In contrast, the erosion yields differ up to a factor of two for the different CFC-materials. In general, the chemical sputtering yields decrease with increasing ion flux density Γ according to $\Gamma^{-0.6}$ reaching levels below 1% at the highest fluxes. Scanning electron microscopy (SEM) and energy dispersive X-ray analysis (EDX) show preferred erosion in the area between the carbon fibers.

Keywords: High flux; Carbon-based materials; Flux dependence; Chemical sputtering

1. Introduction

Graphite and carbon-based materials are used as plasma facing components in most of the existing magnetic fusion experiments. To handle the high particle and power loads in future devices like ITER, the development of three-dimensional carbon-fiber composites (CFCs) with improved thermo-mechanical properties seems a promising way. However, the erosion of these materials by chemical sputtering via the formation of volatile hydrocarbons is a crucial issue. A saturation and subsequent decrease of chemical erosion at high ion flux densities (above 10^{21} m^{-2} s^{-1}) is expected due to increasing recombination of hydrogen, but there is only a scarce experimental data base at plasma parameters relevant for fusion [1, 2, 3].

The plasma generator PSI-1 was used for extensive series of experiments in steady state plasmas to investigate the chemical erosion in this high flux range during the last years. First results were obtained without external control of the target temperature [4]. As a next step the temperature dependence of the chemical erosion yields was studied in detail under controlled conditions [5]. Here, a continuation of this work is presented putting emphasis on the flux dependence of chemical erosion in hydrogen and deuterium plasmas, extended by morphological investigations of the surface modifications. An important aspect is the comparison of two different CFCs with each other and with a common fine grain graphite. Identical experimental conditions

Chemical sputtering yields of carbon based materials at high ion flux densities, H. Grote et al., Journal of Nuclear Materials, 269 (1999) 1059-1064

2

had to be established to get reliable absolute values of the chemical erosion yields.

2. Experiments

A detailed description of the experimental set-up was given in Ref. [5]. The same set of diagnostics was used for this work with some improvements.

2.1. Plasma parameters

In the experiments under discussion the enhancement of the ion flux density was performed by increasing the discharge power. This by its own however, causes also a rise of both the electron temperature and density. Controlling the neutral gas pressure to stay at a constant level allows to keep the temperature low and almost constant and only the density is rising with increasing power input. The radial profiles of electron density and temperature were routinely measured by a reciprocating Langmuir probe in front of the target and confirmed by measuring the ion saturation current onto the target (replacing a molybdenum target instead of the CFCs). These latter measurements were systematically performed, thereby changing the target diameter, covering the mantle of the cylindrical target and/or the back with ceramics or exposing the downstream side only to the plasma.

The electron density n_e was varied between (0.05 and 2.5) $\times 10^{18}$ m^{-3}, the electron temperature T_e was kept at about 5–10 eV, in order to realize a particle impact energy onto the samples of less than 30 eV, i.e. below or near the threshold for physical sputtering [6]. Higher density values are usually correlated with the higher temperatures. So the ion flux density was varied in the range (0.1–5) $\times 10^{22}$ m^{-2} s^{-1}.

2.2. Samples and exposure conditions

CFC-samples of CONCEPT II (DUNLOP) and NS 31 (SEP) – 10% silicon-doped – as well as fine grain graphite EK 98 (Ringsdorff–Werke GmbH) – for comparison – were exposed to hydrogen and deuterium plasmas after appropriate cleaning and outgassing procedures.

Fig. 1 (taken from Ref. [5]) shows the temperature dependence of the erosion yields at an H$^+$-ion flux density of 1.2×10^{22} m^{-2} s^{-1} for the two CFC-materials mentioned above. Here the figure is included to illustrate the method of the measurements at various flux densities. The curves with the solid symbols were recorded with the mass spectrometer (m/e=16, CH$^+_4$) during temperature rise of the samples. The non-calibrated curve with the triangles shows the CH-band intensity during temperature rise of the sample; normalized to the value of the mass spectrometer it exhibits a similar evolution with temperature as the CH$^+_4$ signal. The corresponding open symbols represent the values derived from mass loss measurements after long term exposure at constant temperature for both materials. The abscissa represents the start-up of the exposure time, when the specimen is heated up by the plasma. Starting the exposure at room temperature one gets the maximum value during temperature rise for each flux density and high signals during the long term exposure, carried out at sample surface temperatures slightly

beyond the maximum for chemical sputtering. The erosion yield values given in this paper are corrected with respect to the measured values at constant sample temperature to the maximum values according to Fig. 1.
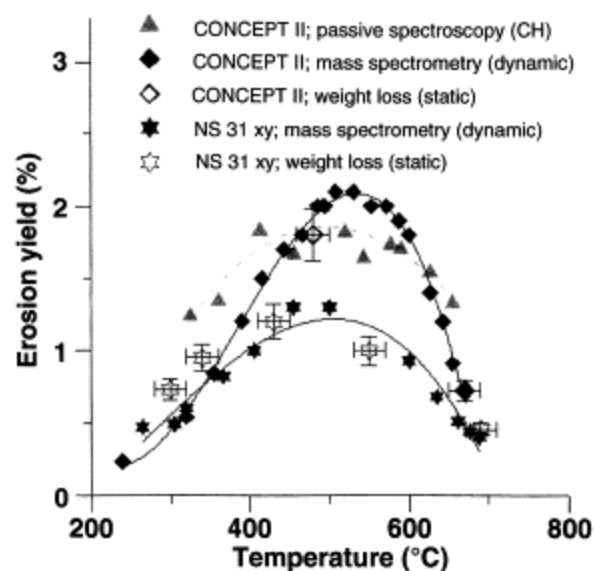

Fig. 1. Temperature dependence of the chemical erosion yield at an H+-ion flux density of 1.2 × 1022 m-2 s-1.

2.3. Diagnostics

The sample exposure time was set to 120 min. This long exposure time was necessary in particular to determine the loss of mass. The temperature of the samples was actively controlled using a gas cooled sample holder equipped with an attached thermocouple. The surface temperature was monitored by a pyrometer; its local distribution was measured using IR-thermography. It passed the maximum for chemical sputtering (Fig. 1), reached 580–630°C about 15 min after the beginning of the exposure and was fixed at this level by active cooling. During temperature rise and the whole exposure time the axial dependence of the CH- (CD-) band intensity at 431 nm and the Hγ- (Dγ-) line were measured with up to 8 channels in front of the sample (5–30 mm). The CH- (CD-) intensity appeared to be independent of position and can thus be taken as a measure of the CH- (CD-) density. The analysis then used the ratio $\int$(CH) dλ /$\int$(Hγ) dλ or $\int$(CD) dλ/$\int$(Dγ) dλ to compensate for possible transmission changes. Furthermore, the C$_x$H$_y$- (C$_x$D$_y$-) formation was monitored by using a differentially pumped gas analyzer. To reduce the background, the amount of graphite exposed to the plasma was minimized – the neutralizer plate was made of tungsten, apertures were covered with tungsten foils, only the cathode heater is made of graphite.

In addition to the in situ methods weight loss measurements and scans with an optical profilometer over the etched crater area were carried out to determine the eroded mass. Finally, surface analysis methods (SIMS, AES, SEM and EDX) were used to check for possible impurities deposited on the sam-

Chemical sputtering yields of carbon based materials at high ion flux densities, H. Grote et al., Journal of Nuclear Materials, 269 (1999) 1059-1064

3

ple surface and to detect morphological changes. The morphology of the surface of the samples was investigated using SEM (Hitachi-S4000) at a voltage of 2 and 20 kV. The EDX-measurements were taken with EDAX DX-4, usually at 5 and 20 kV.

2.4. Calibration

The in situ methods – optical diagnostic and mass spectrometry – were calibrated for each ion flux density with the known fluxes of CH_4 (CD_4), the main product of chemical erosion [5]. These gases were blown into the discharge either through a hole in a molybdenum target or through a nozzle near the target under almost identical conditions as for the graphite sample exposure. This is a direct calibration because no assumptions concerning photon efficiencies and fractions of hydrocarbons reaching the mass spectrometer have to be taken into account. Fluxes exceeding 4×10^{16} s^{-1} were achieved using mass flow controllers, lower fluxes were realized using a small nozzle (diam. 10 μm) and varying the pressure in a reservoir (50–200 mbar). The calibration curves are approximately linear in the interesting range of fluxes e.g. 4×10^{16} particles/s correspond to an erosion yield of about 1% at an H-ion flux density of 1×10^{22} m^{-2} s^{-1}.

3. Results and discussion

The chemical erosion yields for two types of CFC-materials (DUNLOP-CONCEPT II and silicon-doped SEP NS 31) were determined in hydrogen and deuterium plasmas for ion flux densities of $(0.1–5) \times 10^{22}$ m^{-2} s^{-1}. They are compared with fine grain graphite EK 98, commonly used in existing fusion experiments.

The following figures display distinct features of the overall behavior. Fig. 2 shows experimental data for CFC CONCEPT II. The points marked with solid symbols represent exposures in hydrogen plasmas whereas the open symbols are those for deuterium. Within the error bars of the three different methods of analysis there is no difference between the erosion yields in hydrogen and deuterium. Therefore, in what follows we will not distinguish between exposures in hydrogen and deuterium.
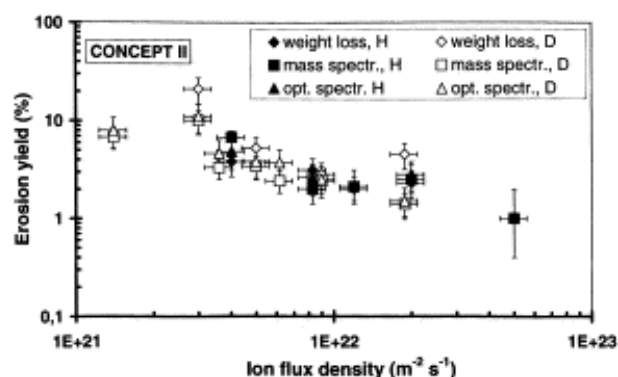

Fig. 2. Dependence of the chemical erosion yield on the incident ion flux density for DUNLOP CONCEPT II. Solid symbols show exposures in hydrogen, open symbols represent deuterium discharges.

The scattering of the individual methods around the average value for the erosion yield is shown for CFC NS 31 in Fig. 3. Within 40% of the average value more than 90% of all single measurements are found. The decrease of the erosion yield with incoming ion flux density is fitted by a power law of $Y \propto \Gamma^{-0.6}$.
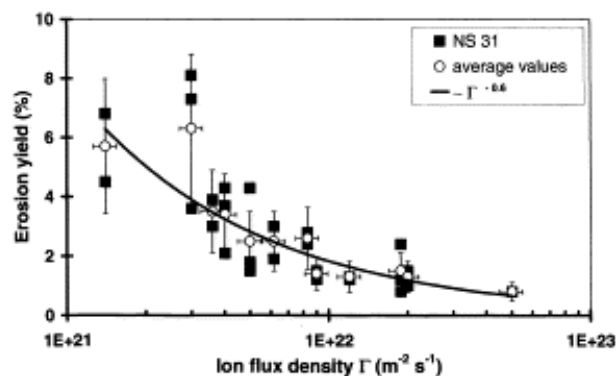

Fig. 3. The chemical erosion yield as a function of the incident ion flux density for SEP NS 31. Open symbols represent average values calculated from the three experimental methods (solid symbols).

The differences in the erosion yields for the investigated specimen are shown in Fig. 4. The decrease with increasing ion flux density is the same for all materials indicating the same underlying physical effect. The erosion values for the silicon-doped CFC NS 31 are generally lower than for CONCEPT II and reach values below 1% at the highest flux densities investigated. The values for EK 98 are almost identical with NS 31 and therefore difficult to distinguish in the figure. The data at 3×10^{21} m^{-2} s^{-1} show an unusual large deviation from the overall trend for both CFC-materials. These were the first in a series of experiments and are possibly erroneous due to plasma impurities or poor sample conditioning. Therefore three additional measurements were carried out to proof these data, resulting in the data points at 1.4, 3.6 and 6.2×10^{21} m^{-2} s^{-1}, that fit the overall trend very well.

EDX-spectra and SEM micrographs were taken in a marked area of every sample before and after exposing the samples to plasma. Particles from materials different than C (and Si in the Si-doped sample) substantiated on the surface before plasma exposure disappeared after plasma exposure; then the EDX-spectra only showed C (and Si). The detection limit of the EDX-method amounts to 1% of the total measuring volume. Any possible a-C:H-layers on the surface are not resolved by SEM.

Fig. 5(a) shows the surface of a CFC-sample (CONCEPT II) before exposure to the plasma. The C-matrix consists of layers and the cut of the C-fiber is shaped like a star. After exposure to the plasma (Fig. 5(b)) the erosion of the C-matrix is clearly seen; a typical structure resulting from chemical etching is established: The fibers are etched to different conical shapes possibly attributed to various initial surface conditions. There is a preferential erosion of the

Chemical sputtering yields of carbon based materials at high ion flux densities, H. Grote et al., Journal of Nuclear Materials, 269 (1999) 1059-1064

4

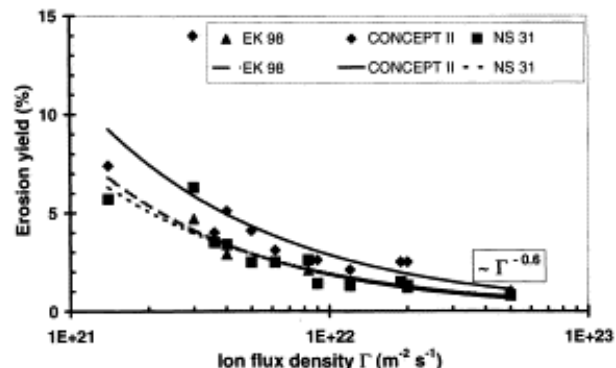amorphous C-matrix and of the transition region between matrix and fiber.

Fig. 4. Chemical erosion yield vs. incident ion flux density for three different materials.
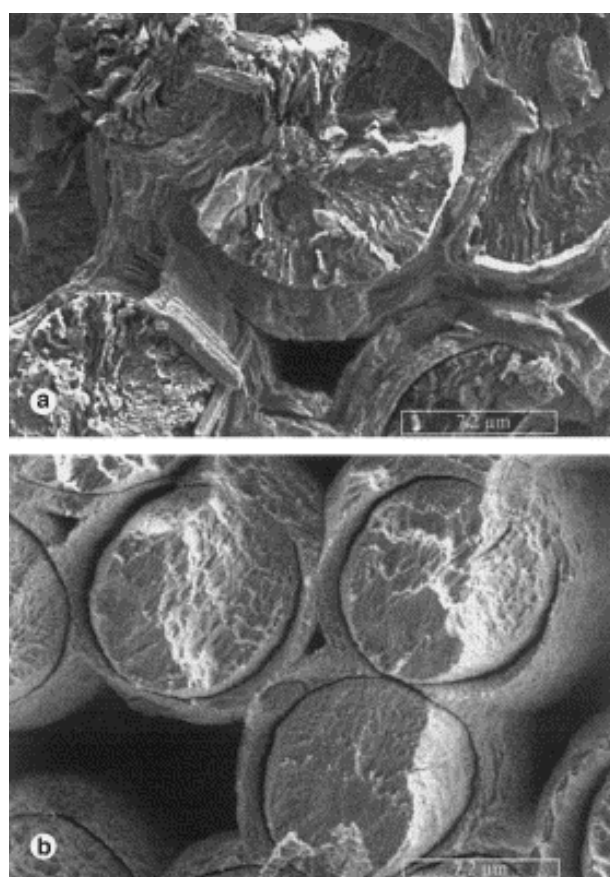

Fig. 5. SEM image of CONCEPT II (a) before exposure and (b) after exposure.

In Fig. 6 the etched surface of a graphite fiber (NS 31) after exposure is shown. This micrograph exhibits the typical structure of graphite. Here the erosion took place on lattice defects, whereas zones with perfect lattice structure were less affected. A similar pattern of chemical erosion is seen at the fibers of CONCEPT II and on the EK 98 sample.

Due to the silicon between the fibers the morphology of the Si-doped material is different before and especially after exposure to the plasma. There is also a preferential erosion of the amorphous C-matrix, within the matrix/fiber transition zone and on areas of lattice defects of the graphite.

However, since Si and SiC are sputtered physically only, we observe an enrichment of silicon on the surface after exposure. A further reason for the formation of Si-enriched layers may be caused by the heating of the samples [7].
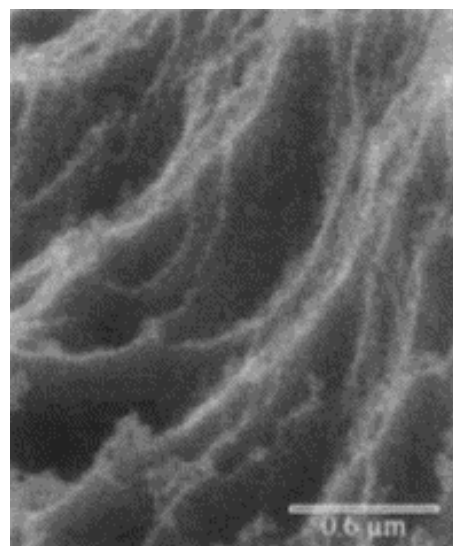

Fig. 6. SEM image of a graphite fiber (NS 31) after exposure.

The steep decrease of the erosion yield is in good agreement with experiments at TEXTOR [2, 8] and ASDEX-Upgrade [9]. The differences in the absolute values can be explained by the lower surface temperature at ASDEX-Upgrade. The measurements at TEXTOR give only the flux ratio Φ $(CD_4)/\Phi(D)$ rather than erosion yields. According to the model developed by Küppers and co-workers [10] and the analytic description of the flux dependence of chemical erosion by Roth and García-Rosales [11, 12] chemical erosion of graphite by hydrogen isotopes results from two processes: the thermal release of hydrocarbons (Y_{therm}) and a kinetic ejection of weakly bound hydrocarbons on the surface due to collisional energy transfer (Y_{surf}). The formula by Roth and García-Rosales [11, 12] predicts a remarkable decrease of the erosion yield just for the range of ion flux densities investigated here. Nevertheless the theoretical slope is still too small compared to our experimental results (Fig. 7). According to the model Y_{therm} and Y_{surf} give almost equal contributions to the total erosion yield. A significant contribution of Y_{surf}, however, would result in a dependence of erosion on the mass of the incident particles. The lacking isotope effect in our measurements is therefore also in disagreement with the model.

The differences in the erosion yields may be explained as follows: Preferential erosion is observed at crystal imperfections or amorphous areas in the CFCs. This generally leads to higher erosion rates of the composites compared to crystalline graphite. The Si-doping partly compensates this effect, so that the erosion rate of the silicon-doped CFC NS 31 is similar to that of EK 98. To reduce the erosion yield of doped CFCs below the values of graphite it seems necessary

Chemical sputtering yields of carbon based materials at high ion flux densities, H. Grote et al., Journal of Nuclear Materials, 269 (1999) 1059-1064

5

to improve the process of graphitization of the CFC-matrix during manufacturing.
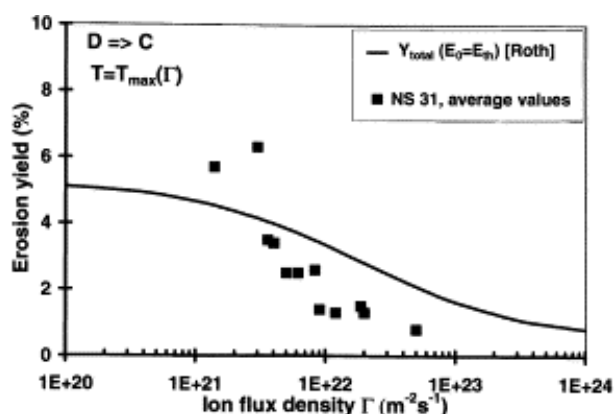

Fig. 7. Total erosion yield vs. ion flux density. Comparison of experimental data with the analytical expression given by Roth and García-Rosales [11, 12].

Possible sources of errors in the determination of the erosion yields are the impact contributions of neutral atoms and molecular ions. Furthermore impurity sputtering as well as redeposition of eroded material must be taken into consideration. The latter effect is particularly critical in the case of high n_e and T_e when the eroded material is ionized near to the sample. The difference between total and net erosion would cause the erosion rates determined by the loss of weight method to be systematically smaller than those determined by the other methods. This, however, is not found in our data. Estimations show that for our conditions (plasma parameters, geometry) about 4% of the eroded material will return to the target [13]. Similarly, physical sputtering would cause the loss of weight measurements to show

significantly higher erosion yields than the in situ methods, since the latter do not detect the sputtered carbon. The influence of plasma impurities, especially oxygen, on the erosion rates was already discussed in [5]; it is discarded because of the very low concentration ($n_O/n_e < 10^{-3}$). The impact of molecular ions and neutral atoms additionally to H^+- (D^+-) ions would lead to an increase of the impinging particle flux and hence decrease the effective erosion yield. As far as the ion-neutral density ratio stays constant the general parameter tendencies would be unaffected. The amount of neutral atoms was estimated to ≈20% of the electron density [5], but further investigations will have to be performed to clear this issue.

4. Summary

The chemical erosion yields for two types of CFC-materials (DUNLOP-CONCEPT II and silicon-doped SEP-NS 31) were determined in dependence on the ion flux density in the range $(0.1–5) \times 10^{22}$ m^{-2} s^{-1} for the temperature of maximum chemical erosion.

No differences in the chemical erosion yields between hydrogen and deuterium exposures are found for the various materials. In contrast, the erosion yields differ up to a factor of two for the different CFC-materials, being lower for the silicon-doped material. In general, the chemical sputtering yields decrease with increasing ion flux density proportional to $\Gamma^{-0.6}$ reaching levels below 1% at the highest fluxes.

Scanning electron microscopy (SEM) and energy dispersive X-ray analysis (EDX) suggest preferential erosion in the space between the carbon fibers where the crystal structure is most imperfect.

Further investigations are planned to study a possible dependence on ion fluence and to extend the flux region to values below 10^{21} m^{-2} s^{-1} and above 5×10^{22} m^{-2} s^{-1}.

References

1. E. Vietzke, A.A. Haasz, in: W.O. Hofer, J. Roth (Eds.) Physical Processes of the Interaction of Fusion Plasmas with Solids, Academic Press, Amsterdam, 1996, p. 135
2. J.W. Davis and A.A. Haasz. *J. Nucl. Mater.* 241–243 (1997), p. 37.
3. C.H. Wu and U. Mszanowski. *J. Nucl. Mater.* 218 (1995), p. 293
4. W. Bohmeyer et al., Proc. 22nd EPS Conf. Contr. Fusion and Plasma Phys., Bournemouth 1995, ECA 19C Eur. Phys. Soc., Geneva, 1995, part. II, pp. 297–300
5. H. Grote et al., J. Nucl. Mater. 241–243 (1997) 1152
6. W. Eckstein et al., Sputtering Data, Report IPP 9/82
7. M. Balden et al., J. Nucl. Mater. 258–263 (1998) 740
8. A. Pospieszczyk et al., Proc. 22nd EPS Conf. Contr. Fusion and Plasma Phys., Bournemouth 1995, ECA 19C Eur. Phys. Soc., Geneva, 1995, part. II, pp. 309–312
9. A. Kallenbach et al., these Proceedings
10. M. Wittmann and J. Küppers. *J. Nucl. Mater.* 227 (1996), p. 186.
11. J. Roth and C. García-Rosales. *Nucl. Fusion* 36 (1996), p. 1647.
12. J. Roth and C. García-Rosales. *Nucl. Fusion* 37 (1997), p. 897.
13. D. Naujoks, private communication